An aromatic hydroxylation reaction catalyzed by a two-component FMN-dependent Monooxygenase. The ActVA-ActVB system from Streptomyces coelicolor.

Julien Valton, Marc Fontecave, Thierry Douki, Steven G Kendrew, Vincent Nivière

AN AROMATIC HYDROXYLATION REACTION CATALYZED
BY A TWO-COMPONENT FMN-DEPENDENT MONOOXYGENASE: THE
ACTVA-ACTVB SYSTEM
FROM *STREPTOMYCES COELICOLOR*

Julien Valton[¶], Marc Fontecave[¶], Thierry Douki[†], Steven G. Kendrew[‡] and Vincent Nivière[¶]

[¶] Laboratoire de Chimie et Biochimie des Centres Redox Biologiques, DRDC-CEA/CNRS/Université Joseph Fourier, 17 Avenue des Martyrs, 38054 Grenoble Cedex 9, France; [†] Laboratoire des Lésions des Acides Nucléiques, DRFMC-SCIB, UMR-E3 CEA-UJF, CEA-Grenoble, 17 Avenue des Martyrs, 38054 Grenoble Cedex 9, France; [‡] Biotica Technology Ltd., Essex, UK

Running Title: ActVB-ActVA, a two-component FMN-dependent monooxygenase

Address correspondence to Vincent Nivière, Tel, 33 4 38 78 91 09; Fax, 33 4 38 78 91 24; E-Mail: vniviere@cea.fr or to Marc Fontecave, Tel, 33 4 38 78 91 03; Fax, 33 4 38 78 91 24; E-Mail: mfontecave@cea.fr

The ActVA-ActVB system from *Streptomyces coelicolor* is a two-component flavin-dependent monooxygenase that belongs to an emerging class of enzymes involved in various oxidation reactions in microorganisms. The ActVB component is a NADH:flavin oxidoreductase which provides a reduced FMN to the second component, ActVA the proper monooxygenase. In this work, we demonstrate that the ActVA-ActVB system catalyzes the aromatic monohydroxylation of dihydrokalafungin by molecular oxygen. In the presence of reduced FMN and molecular oxygen, the ActVA active site accommodates and stabilizes an electrophilic flavin FMN-OOH hydroperoxide intermediate species as the oxidant. Surprisingly, we demonstrate that the quinone form of dihydrokalafungin is not oxidized by the ActVA-ActVB system, whereas the corresponding hydroquinone is an excellent substrate. The enantiomer of dihydrokalafungin, nanaomycin A, as well as the enantiomer of kalafungin, nanaomycin D, are also substrates in their hydroquinone forms. The previously postulated product of the ActVA-ActVB system, the antibiotic actinorhodin, was not found to be formed during the oxidation reaction.

The two-component flavin-dependent monooxygenases have recently emerged as an important class of enzyme systems involved in biological oxidations (1). They are composed of two enzymes. First, a NAD(P)H:flavin oxidoreductase which catalyzes the reduction of free flavin, Flavin Adenine Dinucleotide (FAD) or Flavin MonoNucleotide (FMN), by reduced pyridine nucleotides, NADPH or NADH (2-7). Second, an oxygenase which binds the resulting free reduced flavin together with the substrate in the active site (8-20). There is a general agreement that the reaction proceeds through an oxidation of the flavin by molecular oxygen to generate a flavin hydroperoxide intermediate (21). This is followed by transfer of a single oxygen atom from the electrophilic peroxide to the substrate, generating the oxidized product of the reaction (21). Therefore in this two-component system, NAD(P)H oxidation and the hydroxylation reaction are catalyzed by separate polypeptides. In all cases, with the exception of luciferase (22), there is no evidence for an interaction between the two components and a channeling mechanism allowing the flavin to travel from one protein to another within a protein complex. Accordingly, in most cases, the oxidoreductase component can be replaced by other flavin reductases, including the non-homologous ones from other organisms (4, 5). The flavin transfer process from the oxidoreductase to the oxygenase is thus simply under thermodynamic control (5, 20).

The most extensively studied oxygenase components so far are those utilizing $FADH_2$ as a cofactor, such as 4-hydroxyphenylacetate monooxygenase (HpaB) from *Escherichia coli* (8) phenol hydroxylase (PheA1) from *Bacillus thermoglucosidaflurescens* (4) and styrene monooxygenase (StyA) from *Pseudomonas fluorescens* (12, 13). In contrast, the oxygenases utilizing $FMNH_2$ (termed FMN_{red} herein) have

been much less investigated. Examples are those involved in the synthesis of the antibiotic pristinamycin in *Streptomyces pristinaespiralis* (14, 15), utilization of sulfur from aliphatic sulfonates in *Escherichia coli* (18) or desulfurization of fossil fuels by *Rhodococcus* species (19). In our laboratory, we have been investigating the FMN-dependent two-component enzyme system, consisting of ActVB (6), the flavin reductase, and ActVA-Orf5 (termed ActVA herein) (20), the oxygenase, thought to participate in the last steps of the biosynthesis of the antibiotic actinorhodin in *Streptomyces coelicolor* (23-25) (Scheme 1). Our results have provided new insights into the mechanism of the reaction, especially regarding flavin reduction as well as flavin transfer from the oxidoreductase to the oxygenase (20). The reaction catalyzed by this enzyme system is particularly interesting and might have broader synthetic applications and thus further studies of the mechanism, substrate specificity and reaction efficiency are highly relevant.

Here we report the results of our enzyme assays of the ActVB-ActVA system using the presumed natural substrate dihydrokalafungin (DHK)[1] (23). Unexpectedly, we demonstrate that the DHK substrate appears to be utilized in its hydroquinone form and the only product formed is hydroxylated DHK. Although this enzyme system (or at least ActVB) was originally proposed to be involved in the dimerisation to form actinorhodin (23), we have not so far observed dimerisation under the range of conditions used in our *in vitro* experiments. We also provide further evidence for the involvement of a FMN-OOH intermediate during the catalytic cycle, which is unusually stabilized by the active site of ActVA.

EXPERIMENTAL PROCEDURES

Materials. FMN, NADH and Nanaomycin A (NNM-A) were purchased from Sigma or Aldrich. Other reagent-grade chemicals were obtained from Euromedex. Deazaflavin (5-Deaza-5-carbariboflavin) was a gift from Dr. Philippe Simon (Grenoble, France). Nanaomycin D (NNM-D), dihydrokalafungin (DHK) and actinorhodin were gift to SGK from Professors E. N. G. Marsh, D. Hopwood and S. Omura. Recombinants ActVA-Orf 5 and His tagged ActVB were overexpressed in *E. coli* and purified as described in (6, 20).

Anaerobic procedures. Anaerobic experiments were performed at 18°C in a Jacomex glove box equipped with a UV-visible cell coupled to an Uvikon XL spectrophotometer by optical fibers (Photonetics system). All the solutions were incubated anaerobically for 2 h before the beginning of each experiment.

Preparation of reduced FMN and reduced pyronaphthoquinone substrates. Deoxygenated stock solutions (500 μM) of FMN (ε_{445nm} = 12.5 mM^{-1} cm^{-1}), NNM-A, NNM-D and DHK were anaerobically photoreduced in the presence of 0.5 μM deazaflavin and 10 mM EDTA by irradiation for 30 minutes using a commercial slide projector placed at a distance of 3 cm. The reduced solutions were used within a day.

Oxygenation of pyronaphthoquinone substrates by the ActVA-FMN$_{red}$/O$_2$ system. (i) With reduced pyronaphthoquinone substrates. 10 μM of FMN$_{red}$ was first mixed in the anaerobic glove box with 10 μM of reduced pyronaphthoquinone and 50 μM ActVA into a 100 μl air-tight spectrophotometric cuvette. The oxidation was initiated by the addition of 10 μl of pure oxygen saturated water (1 mM O$_2$) with an Hamilton syringe. The reaction was followed by UV-visible spectroscopy. At the end of the reaction, the mixture was immediately analyzed by HPLC-MS as described below. (ii) With oxidized pyronaphthoquinone substrates. Various amounts of pure oxygen saturated water (1 mM O$_2$) were added to an air-tight micro vial (150 μL) containing 100 μM of oxidized pyronaphthoquinone (final concentration) to a final volume of 100 μL. Oxygen final concentrations ranging between 28 to 90 μM were obtained with this procedure. In the anaerobic glove box, 10 μl of this mixture was injected with a Hamilton syringe into an air-tight spectrophotometric cuvette containing 100 μL of 10 to 20 μM FMN$_{red}$ and 50 μM ActVA solution. The reaction was followed spectrophotometrically. At the end of the reaction, the mixture was analyzed and quantified by HPLC as described below.

Oxidation reaction catalyzed by the ActVB-ActVA system. (i) In the absence of pyronaphthoquinone substrate. Under aerobic conditions, ActVB (155 nM) was added to a mixture containing 200 μM NADH, 46 or 80 μM FMN, 0 to 104 μM ActVA and 20 mM Tris-HCl pH 7.6 in a final volume of 100 μL. The reaction was monitored spectrophotometrically at 25°C. (ii) In the presence of oxidized pyronaphthoquinone substrate. Under aerobic conditions, ActVB (155 nM) was added to a mixture containing 200 μM NADH, 4 μM FMN,

2

36 μM oxidized pyronaphthoquinone substrate (DHK or NNM-A), 0 to 180 μM ActVA in a 20 mM Tris-HCl pH 7.6 buffer. The reaction was followed by UV-visible spectrophotometry at 25°C. The appearance of hydroxylated product was monitored at 520 nm and also analyzed by HPLC-MS as described below. Similar experiments were performed with successive additions of NADH (200 μM) in order to obtain a total hydroxylation of the pyronaphthoquinone substrates.

Quinone reductase activity of ActVB. The steady-state kinetic parameters of the nanaomycin A reductase activity of ActVB were determined in the anaerobic glove box at 18°C, by monitoring the quinone reduction at 423 nm ($\varepsilon_{423nm} = 4.0$ mM^{-1} cm^{-1}). Under standard conditions, the reaction mixture contained 200 μM NADH, 50 mM Tris-HCl pH 7.6 and various amounts of NNM-A, in a final volume of 100 μL. The reaction was initiated by the addition of an ActVB solution containing 34 nM FMN (final concentration). Initial velocities were determined from the early linear part of the reaction progress curves and plotted as a function of NNM-A concentrations. Data were fitted according to the Michaelis-Menten equation using the Levenberg-Marquardt algorithm of Kaleidagraph^{TM}.

DHK quinone reduction by ActVA:FMN$_{red}$ complex. 10 μM of FMN$_{red}$ was mixed in an anaerobic glove box with 28 μM of ActVA and 20 mM Tris-HCl pH 7.6 buffer at 18°C. A deoxygenated DHK$_{ox}$ solution was then added rapidly with a Hamilton syringe to a final concentration of 10 μM and the reaction was monitored by UV-Visible spectroscopy.

HPLC and HPLC–MS analysis. HPLC analyses were performed with a 1100 Agilent chromatographic system coupled to a diode array UV–visible spectrophotometer. An aliquot fraction (100 μL) of the reaction mixture was diluted two times with an aqueous solution containing 0.1 % TFA prior to be loaded onto a C18 column (previously equilibrated with 65 % of ultra pure water and 35 % of acetonitrile, both containing 0.1 % TFA). Elution was conducted with a 35 to 100 % acetonitrile (0.1 % TFA) linear gradient at a flow rate of 1 mL/min during 10 min and monitored by UV-visible spectrophotometry between 250 and 900 nm. Pyronaphthoquinone substrates and hydroxylated products were then quantified from the integration of the HPLC peak monitored at 423 and 520 nm respectively.

HPLC-tandem mass spectrometry analyses were performed with a 1100 Agilent chromatographic system coupled to an API 3000 triple quadripolar apparatus (Applied Biosystem/SCIEX) equipped with a turbo ionspray electrospray source used in the negative mode. Samples were loaded onto a 2 x 150 mm octadecylsilyl silica gel (5 μm particle size) column (Uptisphere, Interchim Montluçon, France) previously equilibrated with 65 % of ultra pure water containing 2 mM ammoniumformate and 35 % of acetonitrile. Elution was carried out with a 35 to 100 % acetonitrile linear gradient in 2 mM ammonium formate as the mobile phase, at a flow rate of 200 μL/min during 10 min. Mass analyses were performed in the multiple reaction monitoring mode (MRM). For this purpose, fragments corresponding to the decarboxylated ([M-44-H]) pseudo-molecular ions were quantified. The transitions corresponding to pyronaphthoquinone, hydroxylated pyronaphthoquinone and actinorhodin were monitored simultaneously with a dwell time set at 650 ms for each compounds.

RESULTS

The ActVA-ActVB system in the absence of pyronaphthoquinone substrates: evidence for a flavin-hydroperoxide intermediate under steady-state conditions.

In the experiments described below, the complete flavin reductase (ActVB)-monooxygenase (ActVA) system was investigated in the absence of pyronaphthoquinone substrates under aerobic ([O$_2$] = 200 μM) steady-state conditions. An excess of ActVA with regard to both ActVB and FMN was used in order to ensure that the reduced flavins (FMN$_{red}$) produced by the action of ActVB/NADH were fully trapped within ActVA polypeptide chains (in agreement with the previously determined K_d values for FMN$_{red}$ with regard to ActVA and ActVB, 0.39 μM and 6.60 μM respectively (20)). Furthermore the FMN concentration was such that the ActVB enzyme was saturated (K_m value for FMN$_{ox}$ = 1 μM (6)). The reaction could be monitored by UV-visible spectroscopy since both NADH and FMN are characterized by specific light absorption bands in the 300-500 nm region. NADH (200 μM) oxidation was monitored at 340 nm whereas FMN$_{ox}$ reduction was followed at 445 nm. The results are shown in Figure 1. During the first step of the aerobic incubation,

we observed an oxidation of NADH (decrease of the intensity of the 340 nm band) which stopped (plateau of the intensity at 340 nm) after approximately 100 seconds, when all NADH was consumed (Figure 1A). During the first 100 seconds, FMN_{ox} was transformed (decrease of the intensity at 445 nm) almost quantitatively into a species whose concentration remained constant (plateau at 445 nm) as long as NADH was present in solution (Figure 1A). During this steady-state, FMN was mostly in a state displaying a single absorption band at 370 nm in the UV-visible spectrum (the slight absorption above 450 nm corresponds to the residual FMN_{ox} form), characteristic for a flavin-hydroperoxide species (21), FMN-OOH (Figure 1B, squares). After 100 seconds reaction, when all NADH was oxidized, the flavin was slowly and totally converted back to FMN_{ox}, as shown from the increase of the intensity of the 445 nm absorption band (Figures 1A and 1B). From Figure 1A, a first order rate constant of $k = 0.84$ min^{-1} was determined for the decomposition of the FMN-OOH species. This process (100-359 seconds reaction time) occurred without any absorbing intermediate species, since spectral changes involved three isobestic points at 333, 365 and 399 nm (Figure 1B). Note that the first spectrum at 76 s does not share all these isobestic points since it also contains absorption at 340 nm due to residual NADH. This experiment showed that, in the absence of substrate and under the reductive pressure of NADH, the intermediate FMN-OOH is present in aerobiosis under large steady-state concentrations and is thus spectrophotometrically observable.

The same type of experiment was carried out with various concentrations of ActVA. As shown in Figure 2A, the steady-state level of FMN-OOH, reflected by the plateau of the optical density at 445 nm (reaction time 50-100 seconds), increased with increased ActVA concentration. The amount of FMN_{ox} converted to FMN-OOH was determined from the OD at 445 nm using the difference between its value at the end of the reaction (t > 350 s) and its value at the plateau (t = 50 s), assuming negligible contribution of the FMN-OOH species at this wavelength. It should be noted that in these conditions free FMN_{red} does not accumulate since it is immediately oxidized by the excess of O_2. Plotting this value as a function of ActVA concentration generates a straight line, indicating that FMN-OOH accumulation is directly proportional to ActVA concentration. The slope in Figure 2B gives the amount of FMN-OOH formed per ActVA molecule. The results demonstrated that under the experimental conditions used here, one molecule of FMN-OOH was formed per dimer of ActVA, at the steady state.

The ActVA- ActVB system in the presence of pyronaphthoquinone substrates: a monooxygenation reaction.

The substrate of the enzyme system is presumed to be dihydrokalafungin (DHK, Schemes 1 and 2). However, enzymatic oxidation of DHK has not been shown *in vitro*. When DHK (36 μM) was incubated aerobically with the ActVA-ActVB system in the presence of 4 μM FMN and 200 μM NADH in 20 mM Tris-HCl buffer, pH 7.7, a product was formed at the expense of DHK, as shown by HPLC. No product could be obtained in the absence of ActVA (data not shown). Figure 3A shows the chromatogram detected at the end of the reaction when all NADH has been oxidized (100 seconds). DHK is eluted at 7.4 min and the product at 7.7 min. The spectrum of the product is shown in Figure 3B (triangles). The absorption band enjoys a large bathochromic shift with regard to that of DHK, from 423 to 507 nm and is significantly different from that of actinorhodin. The ε values have been estimated as described below. Analysis of the new compound by LC-MS demonstrated that its mass differed from that of DHK by only one oxygen atom (m/z = 317 Da instead of 301 Da for DHK). This result showed that the product of the reaction *in vitro* was not actinorhodin (m/z = 633 Da), but rather a monooxygenated derivative of DHK, named DHK-OH in the following.

In the experiment of Figure 3, using 200 μM NADH, DHK (36 μM initial concentration) was only partially converted to DHK-OH, as monitored by HPLC. We thus carried out several reaction runs by repeated additions of 200 μM NADH and oxygen until all the DHK was oxidized to product. From one run to the following the spectrum did not change in shape and the area of the peak corresponding to DHK-OH increased by about the same extent to reach a plateau when all DHK was oxidized. Assuming that the only oxidation product under these conditions was DHK-OH and that conversion of DHK to DHK-OH was quantitative, one thus could determine the extinction coefficient for DHK-OH at 507 nm,

with a value of 4.4 mM^{-1} cm^{-1} (as compared to 0.27 mM^{-1} cm^{-1} for DHK). This extinction coefficient of the band at 520 nm for DHK-OH was comparable to that of the band at 423 nm for DHK. This was also observed for quinone analogs such as 5-hydroxy-1,4-naphtoquinone and 5,8-dihydroxy-1,4-naphtoquinone, which display visible spectra remarkably similar to those of DHK and DHK-OH respectively (26).

It was clear that the reaction yield, calculated as the amount of DHK-OH divided by the amount of consumed NADH (200 μM) during the first run, was low. This yield increased with increased ActVA concentration but leveled off at about 10 % with the highest concentrations (Figure 4). The dependence of the yield on FMN concentration was also studied and showed that the optimal concentration of FMN was 4 μM, using 37 μM of ActVA (data not shown).

The same complete study, involving product characterization (UV-visible spectroscopy, mass spectrometry) and calculation of reaction yields, was carried out with NNM-A as a substrate (data not shown). NNM-A is the enantiomer of DHK (Scheme 2). As for DHK, only one monooxygenated product was obtained. Figure 4 shows the dependence of the yield of NNM-A oxygenation upon ActVA concentration, demonstrating that it is a poorer substrate.

Taken together, these results indicated a very inefficient coupling of ActVB (flavin reduction) and ActVA (monooxygenation) activities. A possible source of uncoupling was the unproductive reaction of free FMN$_{red}$ with molecular oxygen during flavin transfer from ActVB to ActVA. However, as a large excess of ActVA was used in our experiments to ensure fast and complete binding of FMN$_{red}$, this factor is unlikely to be a significant contribution to the uncoupling. Another possible source of uncoupling was identified as described below.

Quinone reductase activity of the ActVA-ActVB system.

Reduced flavins are excellent reducing agents with regard to a variety of electron acceptors such as oxygen, ferric complexes and also quinones (27-29). We thus suspected the quinone compounds (DHK, NNM-A) used as substrates of the ActVA-ActVB system to be reduced by the FMN$_{red}$ generated by ActVB. Indeed, free FMN$_{red}$, obtained through ActVB flavin reductase activity or through anaerobic irradiation in the presence of deazaflavin, was shown to quantitatively reduce NNM-A, as

shown from the intensity of the final band at 353 nm, characteristic of its hydroquinone form (data not shown).

We also investigated the quinone reductase activity of an ActVB preparation containing a tightly bound FMN (29) in the absence of free flavin. In order to avoid competition with molecular oxygen, all the experiments were carried out within an anaerobic glove box. When 200 μM NADH was incubated with ActVB containing 34 nM of FMN bound, in Tris buffer pH 7.6, no oxidation of NADH could be detected. Addition of a quinone substrate such as NNM-A in this medium resulted in its fast reduction by NADH, as shown by the decrease of the intensity of the 423 nm absorption band characteristic for the quinone. Figure 5A shows the initial and final UV-visible spectrum in an experiment with NADH (200 μM) in excess with regard to the quinone (130 μM). At the end of the reaction, there is no more quinone as shown from the lack of the band at 423 nm. The absorption band at around 350 nm is a mixture of a band at 340 nm (residual NADH) and a new band at 353 nm, characteristic of the corresponding NNM-A hydroquinone (30). The contribution of the flavin in all these spectra was negligible due to the extremely low concentration of FMN. These results showed that ActVB catalyzes the reduction of quinones such as NNM-A to the corresponding hydroquinone. The quinone reductase activity of ActVB, defined as the initial rate of the reaction determined from the time-dependent decrease of the intensity of the 423 nm band, exhibited a typical Michaelis-Menten dependence on substrate concentration (Figure 5B and Inset of Figure 5B). This allowed to determine the following kinetic parameters for the reduction of NNM-A : k_{cat} = 9.6 ± 0.4 s^{-1} and K_m = 29 ± 6 μM. Taken together, these data clearly show that ActVB is able to catalyze the reduction of quinone compounds at the expense of NADH, through either free flavin or protein bound FMN.

Since ActVA accommodates both FMN$_{red}$ and the substrate into its active site, we reasoned that a quinone substrate might, as an electron acceptor, compete with oxygen for reaction with FMN$_{red}$. Figure 6 shows the initial spectrum of a solution containing 28 μM of ActVA and 10 μM of FMN$_{red}$, in which FMN$_{red}$ is fully complexed (20) and the final (0.5 min reaction) spectrum after addition of 10 μM DHK. The spectrum indicates formation of FMN$_{ox}$ (by the presence of the band at 450 nm) and of the hydroquinone

form of DHK (by the band at 353 nm). Since FMN_{red} is fully complexed to ActVA, direct reduction of DHK_{ox} by free flavin is unlikely. The intensity of the 450 nm band allows us to calculate that 10 µM of FMN_{ox} was generated, thus showing that the reduction of DHK by FMN_{red} was quantitative. These results demonstrate that an important source of uncoupling between NADH oxidation and substrate monooxygenation might reside in the efficient oxidation of FMN_{red} by the quinone moiety of the substrates within ActVA.

The effect of oxygen.

Based on the observation that in ActVA FMN_{red} reacts with both the quinone substrate and molecular oxygen and on the assumption that only the second process leads to the active oxygenating species, we reasoned that the efficiency of the monooxygenation reaction should be a growing function of molecular oxygen concentration. In order to test this hypothesis, we designed conditions for oxidation of DHK in the absence of ActVB. Using the simplified one-turnover monooxygenating system based on ActVA (50 µM) in excess with regard to FMN_{red} (20 µM) in Tris buffer pH 7.6 prepared in the anaerobic glove box, we investigated the effect of increasing the concentration of oxygen on the efficiency of the monooxygenation of DHK. The reaction was initiated by injecting a solution containing both DHK and oxygen at known concentrations so that the final concentration of DHK was 10 µM and that of oxygen was variable. The reaction was completed within 1 min incubation and was analyzed by HPLC to determine the amount of both residual DHK and DHK-OH. We also checked that under these conditions DHK was converted into a single product which was identified as DHK-OH. Thus, the outcome of the oxidation reaction catalyzed by ActVA was the same whether the reduced flavin was provided as free FMN_{red} (in the absence of ActVB) or by the FMN_{ox}/ActVB/NADH system. However, the dependence on oxygen concentration, shown in Figure 7, was unexpected. Whereas O_2 was absolutely required for the reaction, DHK-OH formation decreased as a function of O_2 concentration above 30 µM. The decrease of DHK-OH at high concentration of O_2 was not due to an overoxidation/decomposition of DHK-OH, since less DHK substrate was consumed at increased O_2 concentration. These results allowed us to hypothesize that the true substrate

of the enzyme was not DHK but the corresponding reduced hydroquinone form which could be formed by reaction of DHK with FMN_{red}. Hydroquinones are well-known as oxygen-sensitive compounds and high concentration of O_2 could inhibit the reaction by decreasing the proportion of DHK in the hydroquinone form. This hypothesis was confirmed experimentally as shown in the next paragraph.

ActVA substrate specificity.

In the following experiments, we used the one-turnover system described above to investigate the substrate specificity of ActVA. Three compounds, DHK, NNM-A and NNM-D (Scheme 2), in either the quinone or hydroquinone forms were tested. The reactions were carried out in the anaerobic glove box and analyzed aerobically by HPLC, monitoring the eluate at 423 nm (substrate) and 520 nm (monooxygenated product). For all experiments, only two peaks were present in the chromatogram, one corresponding to the quinone substrate and the other to the quinone monooxygenated product. This is consistent with the analysis performed aerobically as under these HPLC analysis conditions any hydroquinones are immediately converted to the quinone forms. With quinone substrates the reactions were initiated by addition of an aerated solution (final concentration 100 µM O_2) containing the compound. For the hydroquinones, a reaction mixture containing FMN_{red}, ActVA and the substrate was first prepared in the glove box and the reaction was initiated by addition of an aerated water solution (100 µM O_2 final concentration). The results are shown in Table 1 and establish that the hydroquinones are indeed the substrates of ActVA, with $DHK_{red} > NNM-A_{red} > NNM-D_{red}$ and with an excellent yield for DHK_{red} (90%). Under the same conditions, no oxidation of the corresponding quinones could be observed.

DISCUSSION

The ActVB-ActVA system was investigated in our laboratory as a model for studying the mechanism of the two-component FMN-utilizing monooxygenase. ActVB (flavin reductase) catalyzes the reduction of FMN_{ox} by NADH and ActVA (monooxygenase) uses the resulting FMN_{red}, as a cofactor for activation of molecular oxygen and subsequent substrate oxidation. We are now able to propose an

enzymatic mechanism which involves the following steps (Scheme 3): (i) reduction of free FMN_{ox} into free FMN_{red} by NADH, catalyzed by ActVB; (ii) rapid binding of FMN_{red} by ActVA (K_d value of 0.39 µM); (iii) reaction of FMN_{red} with O_2 within ActVA to generate a semi-stable electrophilic active FMN-OOH species; (iv) binding of the substrate in its hydroquinone form and monooxygenation. The dimerization reaction leading to the formation of actinorhodin does not appear to be catalyzed by the ActVB-ActVA system, at least under any of the conditions we have used here. Then, in *S. coelicolor*, the enzymes involved in the production of actinorhodin remain to be identified.

Previously, we had been able to observe a FMN-OOH species during reaction of ActVA-FMN_{red} with O_2 in the absence of ActVB. Here we show that the same hydroperoxide characterized by a unique band at 370 nm accumulated during aerobic incubation of the complete two-component system ActVB-ActVA in the presence of FMN and NADH but in the absence of substrate, supporting the mechanism shown in Scheme 3. Under the reducing pressure of NADH, the ActVB-ActVA system converts almost all FMN_{ox} into FMN-OOH through reduction to FMN_{red}, followed by rapid oxidation by O_2 within ActVA. Thus substrate binding is not required for formation of the peroxide. FMN-OOH, which is usually considered as a very unstable compound (21), accumulated in ActVA and was maintained at a large concentration under steady-state conditions. It could be detected spectrophotometrically because of: (i) the stabilizing effect of the ActVA protein, (ii) the presence of an excess of NADH, (iii) the absence of substrate which efficiently consumes the peroxide, and (iv) the slow and limiting rate of decomposition of the peroxide, by an undefined pathway, as compared to the rate of FMN-OOH formation.

The enzyme ActVB was originally proposed to be involved in the dimerisation reaction by analysis of the products produced by strains containing lesions in the biosynthetic cluster (23). However, more recent work has characterized this enzyme and close homologs as members of the FMN:NADH oxidoreductase family (2, 6, 20) that act to supply reduced flavins to a partner enzyme potentially catalyzing a hydroxylation. The ActVA genetic locus has long been thought to be involved in the aromatic hydroxylation (31) and ActVA-Orf5

has been shown to accept reduced flavin and be a strong candidate as partner for ActVB (20). In the present work, we were for the first time able to assay this system *in vitro* using the presumed natural substrates. The results of our assays demonstrate that the only product that could be detected *in vitro* is a monomeric hydroxylated product derived from DHK, which has been termed DHK-OH. This was firmly established by mass spectrometry. No formation of actinorhodin or other dimeric forms could be detected under the conditions of our experiments. The UV-visible spectrum of DHK-OH, significantly different from that of actinorhodin, contained a band at 507 nm, red-shifted with regard to the absorption band of DHK (423 nm) and with comparable extinction coefficient. It is similar to that of 5,8-dihydroxy-1,4-naphtoquinone, whereas that of DHK is similar to that of 5-hydroxy-1,4-naphtoquinone (26). It does indicate that the additional oxygen atom has been incorporated into the hydroxylated aromatic ring. It could be in para position with regard to the OH group at the eleven position, although we cannot completely exclude an hydroxylation at the ortho position. The same hydroxylated product was obtained when ActVA utilized a reduced flavin provided either directly as FMN_{red} or enzymatically by the action of the ActVB/NADH/FMN_{ox} system.

The second unexpected observation was that the enzyme substrate appeared to be the hydroquinone form of DHK (DHK_{red}) rather than the corresponding quinone form. Starting from DHK_{red}, the hydroquinone moiety was not recovered in the DHK-OH product simply because the assay mixture was worked up aerobically for analysis and under these conditions, the oxygen-sensitive hydroquinone was immediately converted back to the quinone. The first evidence that DHK was not directly used as the substrate came from the dependence of the yield of the DHK oxidation reaction catalyzed by ActVA-FMN_{red} on oxygen concentration. If DHK would have been the direct substrate, this dependence would have been expected as a growing function of O_2 concentration, in agreement with FMN-OOH being the active species. This behavior was indeed observed experimentally, but only at very low concentrations of O_2. On the contrary, increasing concentrations of oxygen were found to be inhibitory. Since, as shown here (i) DHK_{red} can be efficiently formed by reduction of DHK by ActVA-FMN_{red}, (ii) DHK_{red} is efficiently

hydroxylated by ActVA/FMN_{red}/O_2, and (iii) DHK_{red} is highly oxygen-sensitive, the O_2 dependence curve demonstrated that DHK_{red} was the substrate of ActVA. The observation that no oxidation at all occurred using a large excess of O_2 thus clearly showed that DHK was not a substrate. Thus, the reason why in some experiments one could nevertheless observe formation of DHK-OH in experiments using DHK as a substrate is that the reaction conditions allowed formation of small amounts of DHK_{red} in the active site of ActVA. In these experiments, there is an excess of FMN_{red} with regard to DHK that allows both reduction of DHK to DHK_{red} and formation of the active FMN-OOH species. There is also a small amount of O_2 thus preventing a fast reoxidation of DHK_{red} to DHK. As a consequence, some product is formed, but obviously poor reaction yields were obtained using DHK as the substrate as shown both with the ActVA-FMN_{red} system or the complete ActVB-ActVA-FMN-NADH system (Table 1).

In the latter more complex case, there were several possible sources of uncoupling between NADH oxidation and DHK oxidation, resulting in very low yields of DHK-OH based on NADH utilization. A significant source of uncoupling could reside in the oxidation of FMN_{red} by DHK during transfer of FMN_{red} from ActVB to ActVA. During this transfer, FMN_{red} can also be oxidized by O_2, a reaction which does not produce FMN-OOH (32). Finally as discussed above, FMN_{red} can be consumed to convert DHK into DHK_{red} within the ActVA active site. The curve reporting the reaction yield as a function of ActVA concentration (Figure 4) demonstrated the occurrence of all these effects. At large excesses of ActVA, allowing fast and complete complexation of FMN_{red} by ActVA, the first two uncoupling reactions were negligible. The low yield value at the plateau reflects the importance of reduction of DHK by FMN_{red} within ActVA. Decreasing ActVA concentration resulted in decreased yield, most likely as a consequence of the increasing contribution of the other uncoupling reactions.

That DHK_{red} is a much better substrate than DHK is consistent with the limit resonance forms of DHK_{red} (Scheme 4). They show that electronic density accumulates in the ortho and para positions with regard to the OH group, allowing nucleophilic attack on the electrophilic FMN-OOH species (Scheme 4). This density is much more delocalized into the adjacent cycle in the case of DHK due to the strong electron accepting properties of the quinone.

Finally, ActVA does not seem to be specific for a single substrate, DHK_{red}. We showed in a previous work that ActVA could catalyze the oxidation of 1,5-dihydroanthraquinone (20). Here we show that NNM-A, the enantiomer of DHK, as well as NNM-D, the enantiomer of kalafungin, the lactone analog of DHK, are also substrates in the hydroquinone form. However, DHK is a much better substrate indicating the importance of the pyrane cycle for recognition of this class of substrates by ActVA. In addition, this specificity is consistent with the actinorhodin configuration, 15R, 3S, identical to that of DHK (Scheme 2). It is well established that many tailoring enzymes appear to display considerable substrate flexibility. We are now in a suitable position to further investigate the substrate specificity of ActVA and further studies will aim at evaluating the possibility of using this system, *in vitro* or *in vivo*, for the synthesis of interesting compounds.

In conclusion, this work demonstrates that in *Streptomyces coelicolor* the two-component FMN-NADH dependent ActVA-ActVB system catalyzes the aromatic monohydroxylation of dihydrokalafungin by molecular oxygen, using an electrophilic flavin FMN-OOH hydroperoxide intermediate species as the oxidant (Scheme 3). It is interesting to note that in this enzyme, the FMN-OOH intermediate accumulates in the absence of substrate. In contrast, in flavoprotein hydroxylases, oxygen activation occurs only after substrate binding. This suggests different regulatory mechanisms as proposed in (5). The previously postulated product, the antibiotic actinorhodin, is not formed during this reaction and biosynthesis of actinorhodin itself needs to be reinvestigated. Furthermore we demonstrate that the quinone form of DHK is not oxidized by the ActVA-ActVB system whereas the corresponding hydroquinone DHK_{red} is an excellent substrate (Scheme 4). We speculate that the strongly reducing cellular conditions, including through the ActVB quinone reductase activity reported here, are enough to maintain the substrate in the reduced hydroquinone form *in vivo* and that a good coupling between NADH and substrate oxidation is occurring.

REFERENCES

1. Galan, B., Diaz, E., Prieto, M. A., and Garcia, J. L. (2000) *J. Bacteriol.* **182**, 627-636
2. Kendrew, S. G., Harding, S. E., Hopwood, D. A., and Marsh, E. N. (1995) *J. Biol. Chem.* **270**, 17339-17343
3. Parry, R. J., and Li, W. (1997) *J. Biol Chem.* **272**, 23303-23311
4. Kirchner, U., Westphal, A. H., Muller, R., and van Berkel, W. J. (2003) *J. Biol. Chem.* **278**, 47545-47553
5. Louie, T. M., Xie, X. S., and Xum, L. (2003) *Biochemistry* **42**, 7509-7517
6. Filisetti, L., Fontecave, M., and Nivière, V. (2003) *J. Biol. Chem.* **278**, 296-303
7. van den Heuvel, R. H., Westphal, A. H., Heck, A. J., Walsh, M. A., Rovida, S., van Berkel, W. J., and Mattevi, A. (2004) *J. Biol. Chem.* **279**, 12860-12867
8. Xun, L., and Sandvik, E. R. (2000) *Appl. Environ. Microbiol.* **66**, 481-486
9. Gisi, M. R., and Xun, L. (2003) *J. Bacteriol.* **185**, 2786-2792
10. Xun, L. (1996) *J. Bacteriol.* **178**, 2645-2649
11. Xun, L., and Webster, C. M. (2004) *J. Biol. Chem.* **279**, 6696-6700
12. Beltrametti, F., Marconi, A. M., Bestetti, G., Colombo, C., Galli, E., Ruzzi, M., and Zennaro, E. (1997) *Appl. Environ. Microbiol.* **63**, 2232-2239
13. Panke, S., Witholt, B., Schmid, A., and Wubbolts, M. G. (1998) *Appl. Environ. Microbiol.* **64**, 2032-2043
14. Blanc, V., Lagneaux, D., Didier, P., Gil, P., Lacroix, P., and Crouzet, J. (1995) *J. Bacteriol.* **177**, 5206-5214
15. Thibaut, D., Ratet, N., Bisch, D., Faucher, D., Debussche, L., and Blanche, F. (1995) *J. Bacteriol.* **177**, 5199-5205
16. Bohuslavek, J., Payne, J. W., Liu, Y., Bolton, H., Jr., and Xun, L. (2001) *Appl. Environ. Microbiol.* **67**, 688-695
17. Xu, Y., Mortimer, M. W., Fisher, T. S., Kahn, M. L., Brockman, F. J., and Xun, L. (1997) *J. Bacteriol.* **179**, 1112-1116
18. Eichhorn, E., van der Ploeg, J. R., and Leisinger, T. (1999) *J. Biol. Chem.* **274**, 26639-26646
19. Xi, L., Squires, C. H., Monticello, D. J., and Childs, J. D. (1997) *Biochem. Biophys. Res. Commun.* **230**, 73-75
20. Valton, J., Filisetti, L.; Fontecave, M., and Nivière, V. (2004) *J. Biol. Chem.* **279**, 44362-44369
21. Palfey, B. A., Ballou, D. P., and Massey, V. (1995) *Active Oxygen in Biochemistry*, (Valentine, J. S., Foote, C. S., Greenberg, A., Liebman, J. F., ed) pp. 37-83, Blackie Academic and Professional
22. Jeffers, C. E., Nichols, J. C., and Tu, S.-C. (2003) *Biochemistry* **42**, 529-534
23. Cole, S. P., Rudd, B. A., Hopwood, D. A., Chang, C. J., and Floss, H. G. (1987) *J. Antibiot. (Tokyo)* **40**, 340-347
24. Caballero, J. L., Martinez, E., Malpartida, F., and Hopwood, D. A. (1991) *Mol. Gen. Genet.* **230**, 401-412
25. Fernandez-Moreno, M. A., Martinez, E., Boto, L., Hopwood, D. A., and Malpartida, F. (1992) *J. Biol. Chem.* **267**, 19278-19290
26. Khan, M. S. and Khan, Z. H. (2005) *Spectrochimica Acta Part A* **61**, 777-790
27. Gaudu, P., Touati, D., Nivière, V., and Fontecave, M. (1994) *J. Biol. Chem.* **269**, 8182-8188
28. Fontecave, M., Eliasson, R., and Reichard, P. (1987) *J. Biol. Chem.* **262**, 12325-12331
29. Filisetti, L., Valton, J., Fontecave, M., and Nivière, V. (2005) *FEBS Lett.* **579**, 2817-2820

30. Tanaka, H., Minami-Kakinuma, S., and Omura, S. (1982) *J. Antibiot. (Tokyo)* **35**, 1565-1570

31. Malpartida, F., and Hopwood, D. A. (1986) *Mol. Gen. Genet.* **206**, 66-73

32. Massey, V. (1994) *J. Biol. Chem.* **269**, 22459-22462

FIGURE LEGENDS

Figure 1. A FMN-OOH intermediate in the steady-state: spectrophotometric evidence. 46 µM FMN_{ox} was aerobically incubated with 104 µM ActVA and 200 µM NADH in a 20 mM Tris-HCl buffer pH 7.6 at 25°C. ActVB was added to a final concentration of 155 nM and the reaction was monitored by UV-visible spectrophotometry. (A) Absorbance variations at 340 (solid line) and 445 nm (dotted line) plotted as a function of the reaction time. (B) UV-visible spectra monitored at 76 (□), 121 (○), 135 (△), 180 (◇) and 359 s (◆) after addition of ActVB. The arrows show the isobestic points.

Figure 2. A FMN-OOH intermediate in the steady-state: stoichiometry with regard to ActVA. 80 µM FMN_{ox} was aerobically incubated with 200 µM NADH and various amounts of ActVA in a 20 mM Tris-HCl buffer pH 7.6 at 25°C. ActVB was added to a final concentration of 155 nM and the reaction was monitored by UV-visible spectrophotometry. (A) Absorbance variations at 445 nm plotted as a function of time in the presence of 26 (○), 36 (△), 52 (□), 78 µM (◇) of ActVA. (B) Concentration of FMN-OOH at the steady state as a function of ActVA monomer concentration. A stoichiometry of 0.5 FMN-OOH per ActVA monomer was determined from the slope coefficient.

Figure 3. ActVA-ActVB hydroxylase activity: identification of the hydroxylated product by HPLC-MS and UV-visible spectroscopy. 4 µM of FMN_{ox} was aerobically incubated with 50 µM ActVA, 155 nM ActVB, 36 µM DHK, 200 µM NADH in a 20 mM Tris-HCl buffer pH 7.6 at 25°C. (A) The reaction mixture was analyzed after 100 s by HPLC-tandem mass spectrometry in the multiple reaction monitoring mode set up to analyze DHK and DHK-OH mass in a negative mode. (B) UV-visible spectra of actinorhodin (○), DHK (□) and DHK-OH (△). The ε values of the latter were determined from the steady-state experiments as described in Experimental Procedures.

Figure 4. Hydroxylation reaction yield as a function of ActVA concentration. 4 µM of FMN_{ox} was aerobically incubated with various amounts of ActVA, 155 nM ActVB, 36 µM DHK or NNM-A and 200 µM NADH in a 20 mM Tris-HCl buffer pH 7.6 at 25°C and the reaction was followed spectrophotometrically. The DHK (○) and NNM-A (△) hydroxylation yield ([hydroxylated product formed]\[NADH consumed]) was determined as described in Experimental Procedures.

Figure 5. Nanaomycin A reductase activity of ActVB. 200 µM NADH was anaerobically incubated with various amounts of NNM-A quinone form in a 20 mM Tris-HCl buffer pH 7.6 at 18°C. ActVB and FMN were added to a final concentration of 155 nM and 34 nM respectively and quinone reduction was monitored at 423 nm as a function of time. (A) UV-visible spectra of the mixture recorded before addition of ActVB and FMN (○) and at the end of reaction (□). (B) Michaelis-Menten plot showing the variation of initial velocity of quinone reduction as a function of NNM-A concentration. Data were fitted as described in Experimental Procedures. Inset shows the double reciprocal plot 1/Vi as a function of 1 / [NNM-A]. A K_m value of 29 ± 6 µM and a k_{cat} value of 9.6 ± 0.4 s^{-1} were determined.

Figure 6. DHK reductase activity of ActVA. 10 µM FMN_{red} was anaerobically incubated with 28 µM ActVA in a 20 mM Tris HCl buffer pH 7.6 at 18°C. DHK quinone form was added to a final concentration of 10 µM and the reaction was followed by UV-visible spectroscopy. Are shown the UV-visible spectra observed before the addition of DHK (□) and 35 s after the mixing (○).

Figure 7. Inhibition of ActVA hydroxylase activity by oxygen. 20 µM FMN_{red} was anaerobically incubated with 50 µM ActVA in a 20 mM Tris HCl buffer pH 7.6 at 18°C. The DHK quinone form containing various amounts of oxygen was then added to a final concentration of 10 µM. At the end of reaction, DHK and DHK-OH were separated by HPLC and monitored spectrophotometrically at 423 and 520 nm respectively. The HPLC peak areas of DHK (○) and DHK-OH (●) were integrated and reported as a function of oxygen concentration.

Table 1. Formation of hydroxylated products as a function of the pyronaphthoquinone substrate redox states, quinone (Ox) or hydroquinone (Red) forms.

	DHK		NNM-A		NNM-D	
	Ox	Red	Ox	Red	Ox	Red
Steady-state experiments	10[a]	/	5[a]	/	0[a]	/
One turn-over experiments	0[b]	90[b]	0[b]	30[b]	0[b]	22[b]

[a] with a large excess of ActVA, 155 nM ActVB, 36 µM pyronaphthoquinone substrate, 4 µM FMN, 200 µM NADH, in aerobic conditions.
[b] with 50 µM ActVA, 10 µM substrate, 10 µM FMN and 100 µM O_2.
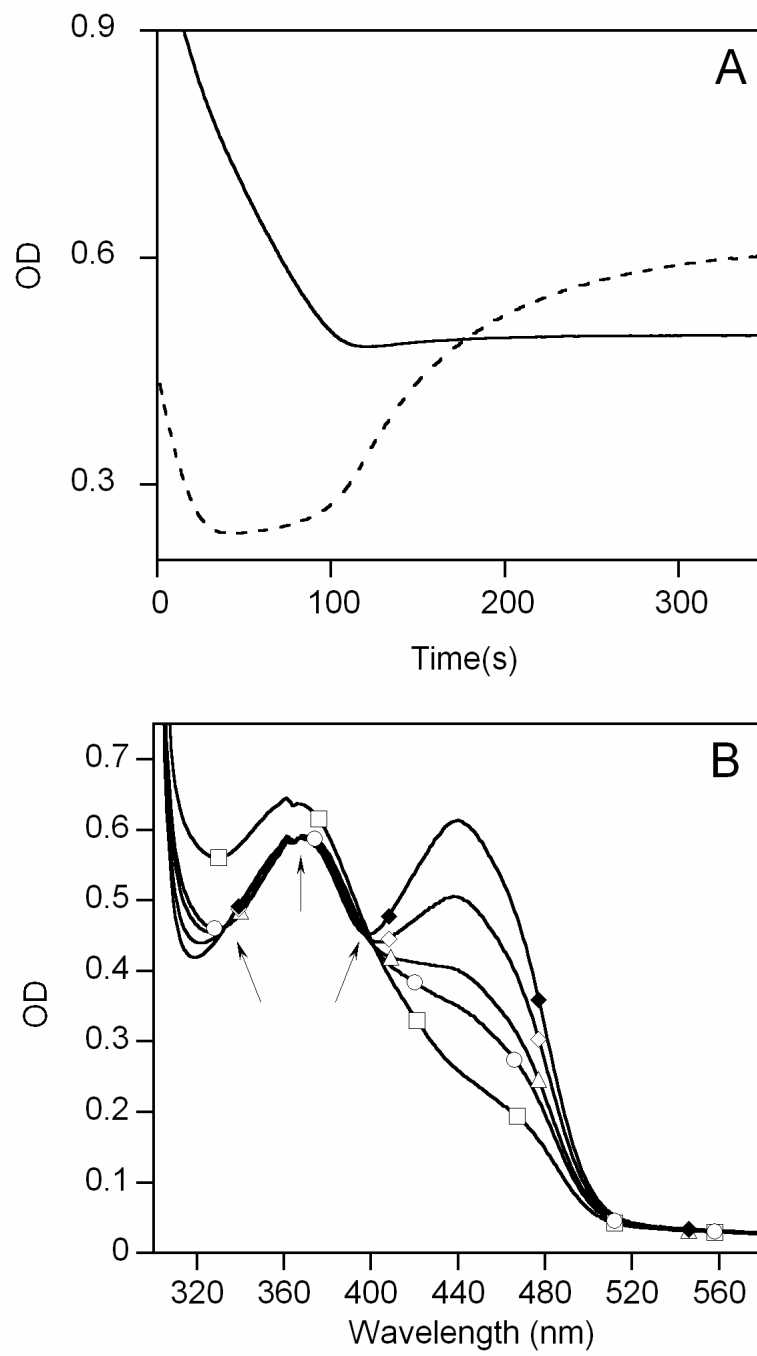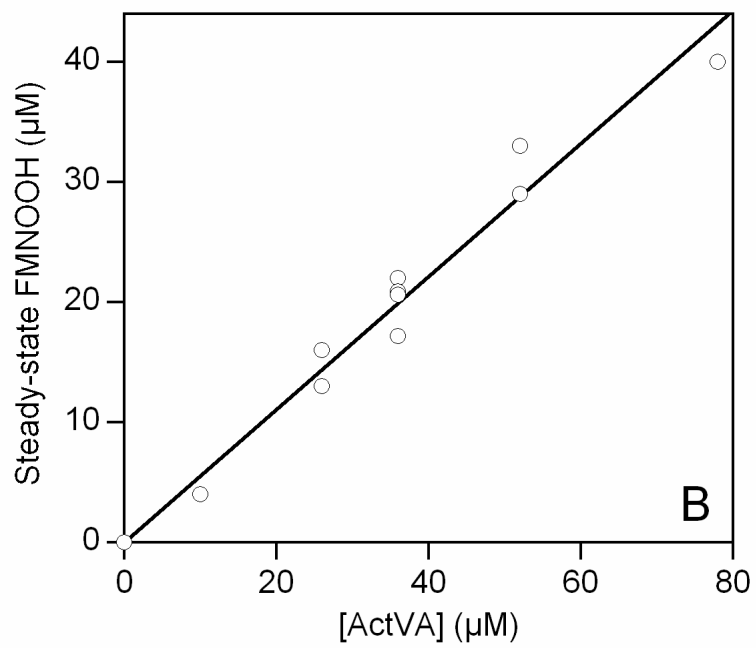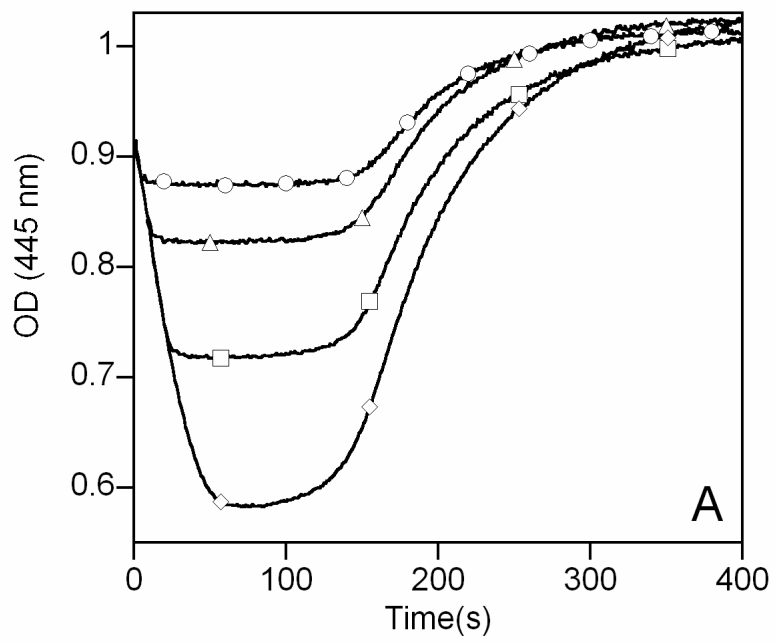
Figure 1

Figure 2
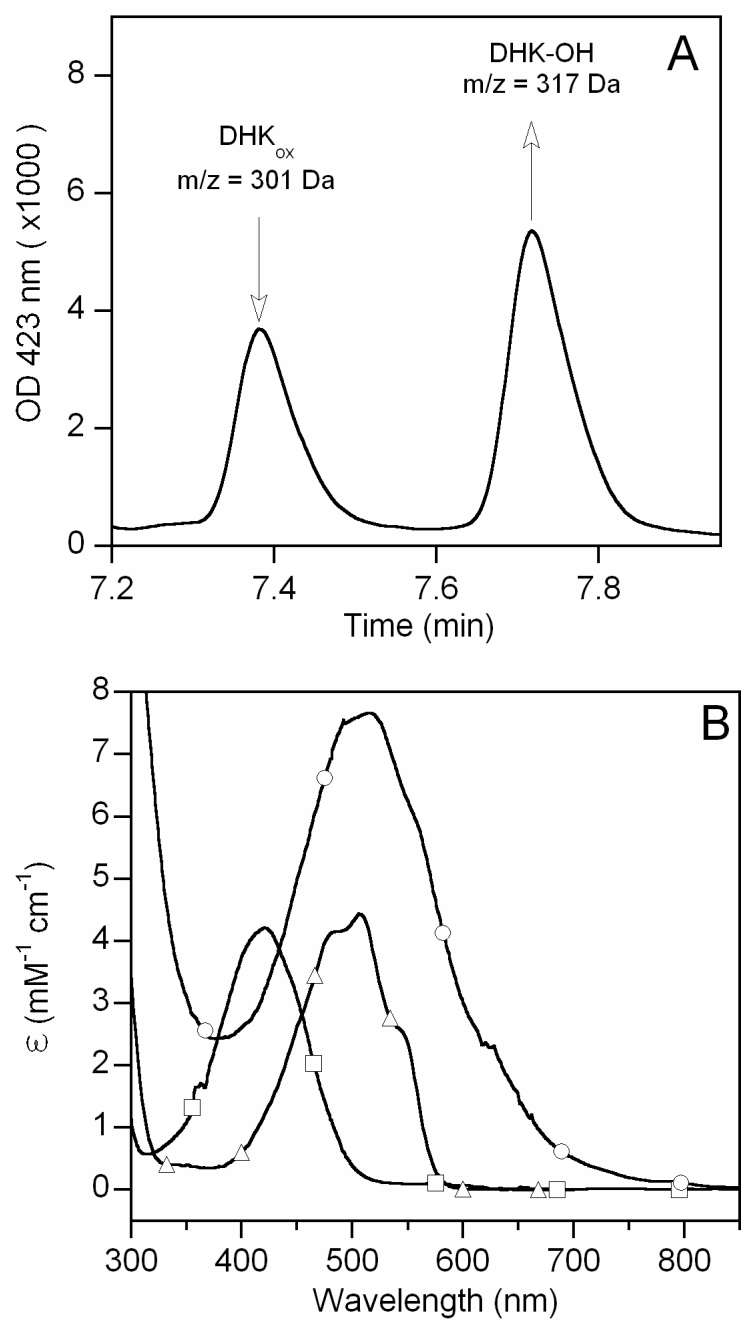
Figure 3
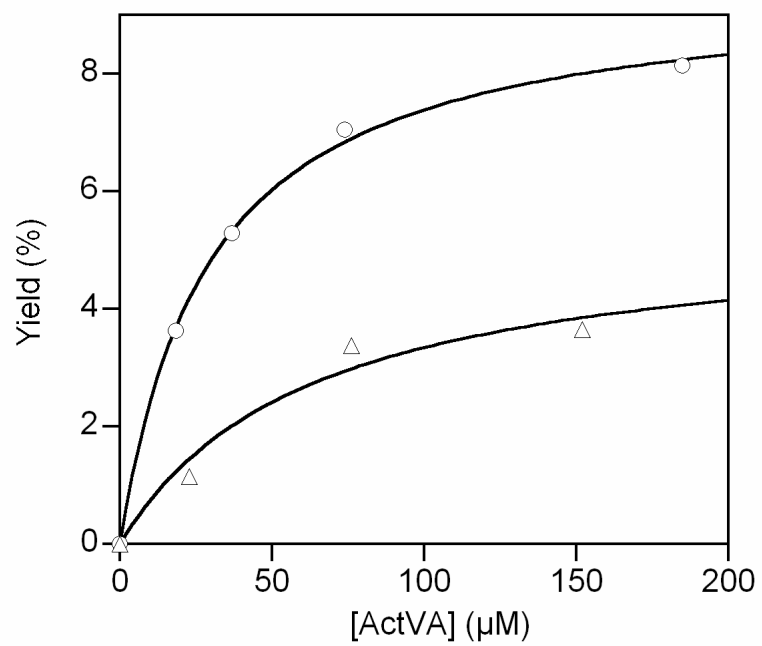
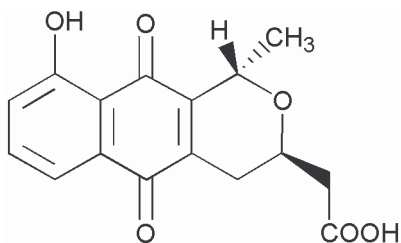Figure 4
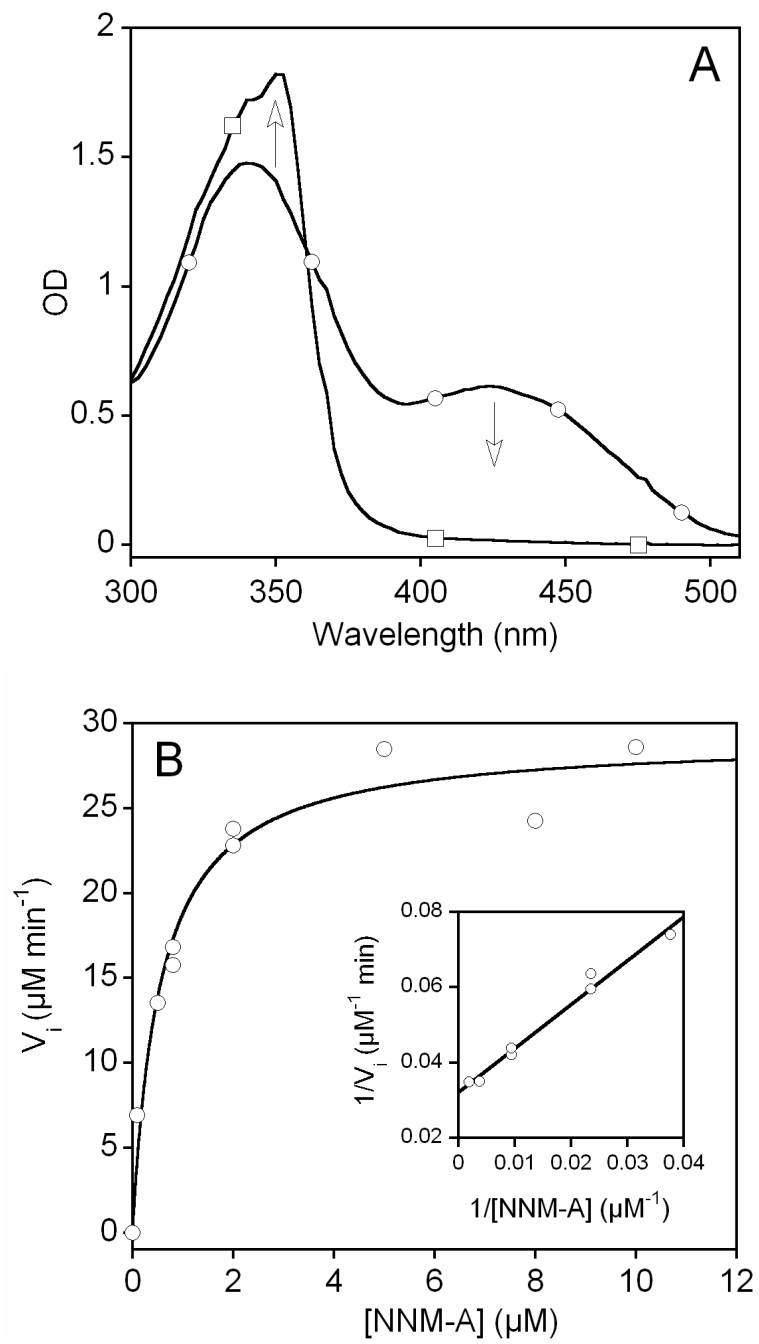
Figure 5
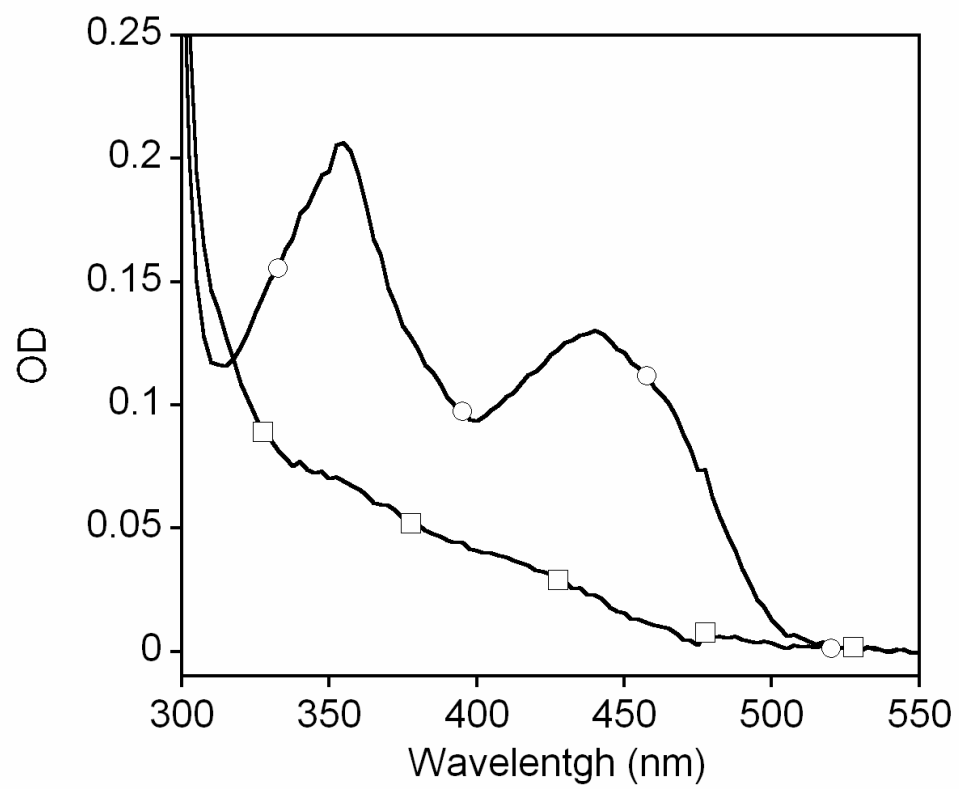
Figure 6
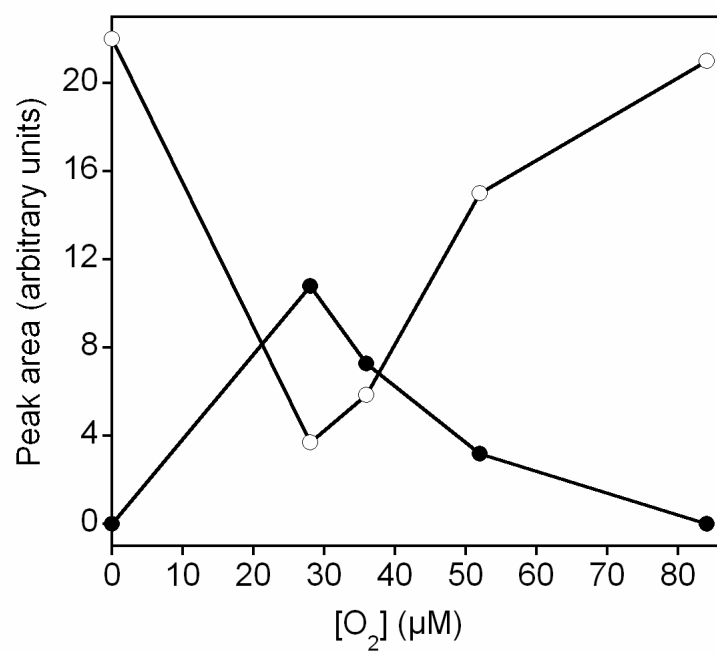
Figure 7
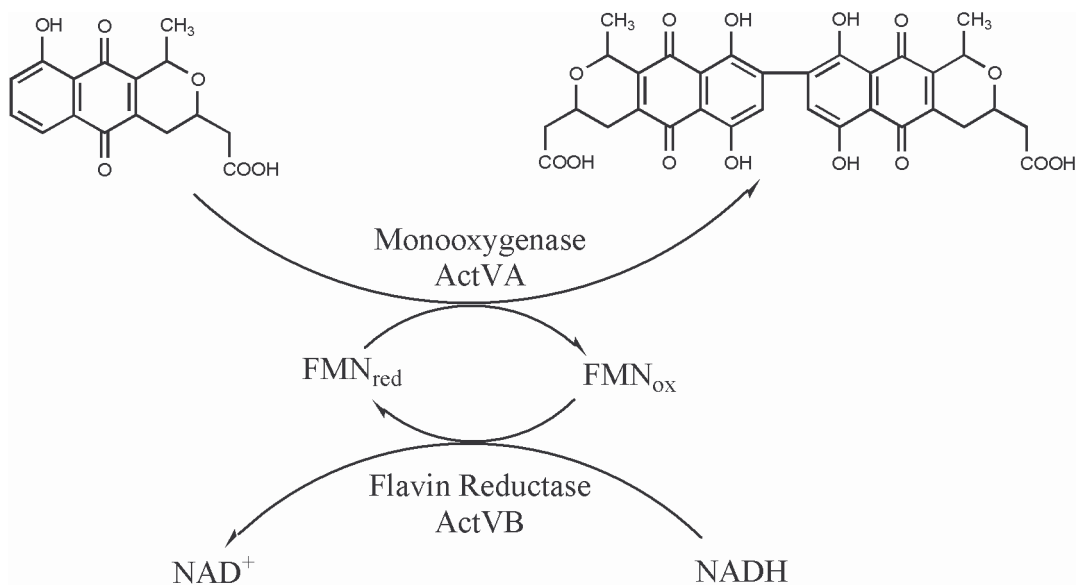
Scheme 1. Actinorhodin as the proposed product of the reaction catalyzed by the ActVB/ActVA system (23).
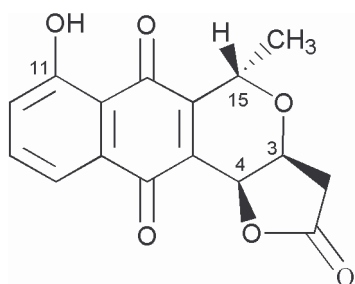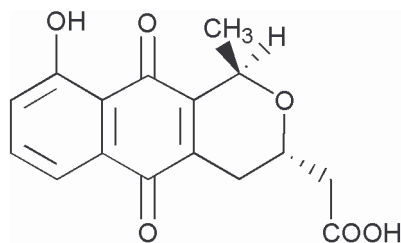
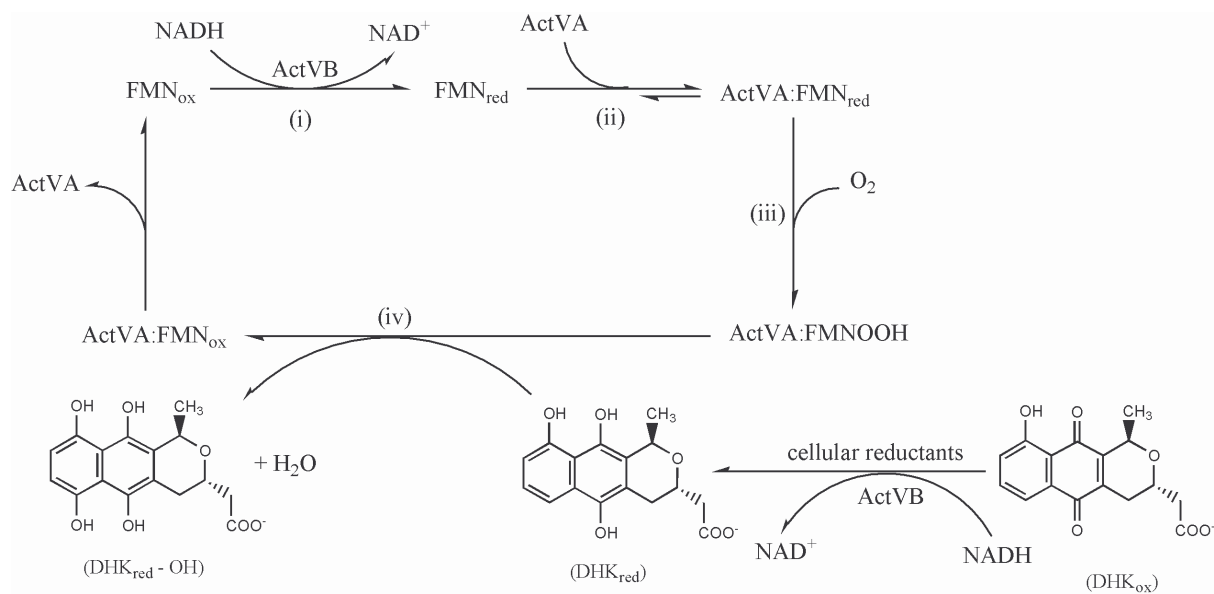NNM-D (15 S, 3 S, 4 S)
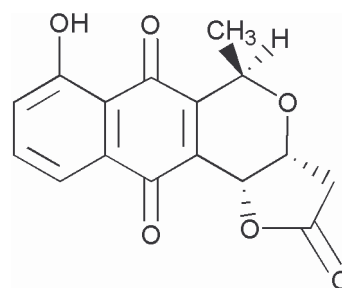
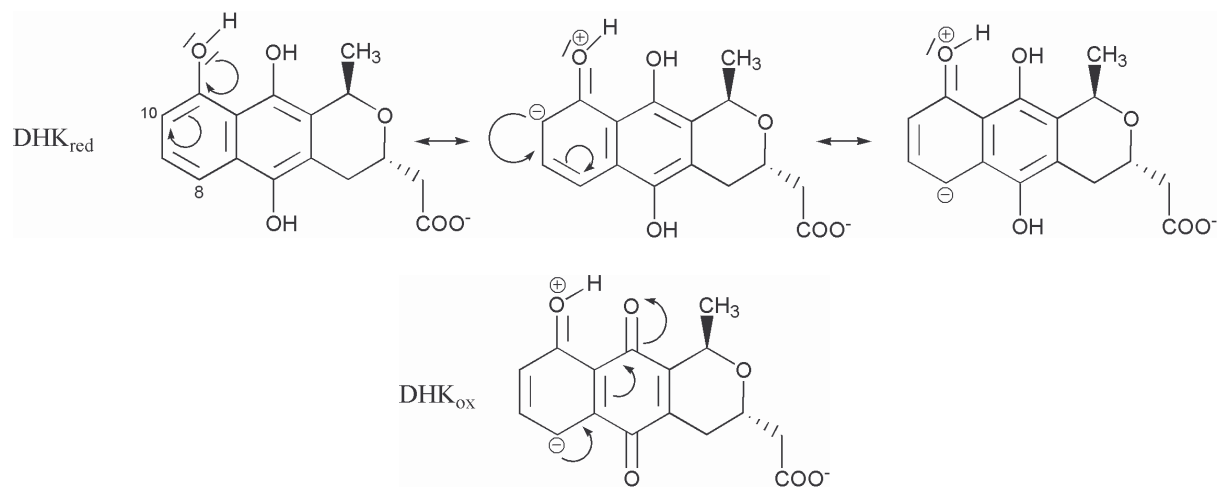Kalafungin (15 R, 3 R, 4 R)

NNM-A (15 S, 3 R)

DHK (15 R, 3 S)

Scheme 2. Structure of pyronaphthoquinone substrates.

Scheme 3. DHK_{red} hydroxylation catalyzed by the ActVA-ActVB system.

Scheme 4. Resonance forms of DHK.